

# Evaluation of Osteoblastic Differentiation Induced by Microtextured Titanium Surface Produced by Laser Metal Fusion 3D Printing

Helena Bacha Lopes<sup>a</sup>, Thiago Leonardo Rios<sup>a</sup>, Leticia Faustino Adolpho<sup>b</sup>,

Alann Thaffarell Portilho de Souza<sup>c</sup>, Ulisses Moreira de Andrade Lopes<sup>d</sup>,

Eduardo Henrique Backes<sup>d,e</sup>, Luiz Antonio Pessan<sup>d,e</sup>, Gileade Pereira Freitas<sup>a,\*</sup> 

<sup>a</sup>Universidade de Cuiabá, Faculdade de Odontologia, Programa de Pós-Graduação em Ciências Odontológicas Integradas, Cuiabá, MT, Brasil.

<sup>b</sup>Universidade de São Paulo, Faculdade de Odontologia de Ribeirão Preto, Bone Research Lab, Ribeirão Preto, SP, Brasil.

<sup>c</sup>Centro Universitário Metropolitano da Amazônia, Faculdade de Odontologia, Belém, PA, Brasil.

<sup>d</sup>Universidade Federal de São Carlos, Programa de Pós-Graduação em Ciência e Engenharia de Materiais, São Carlos, SP, Brasil.

<sup>e</sup>Universidade Federal de São Carlos, Departamento de Engenharia de Materiais, São Carlos, SP, Brasil.

Received: October 12, 2023; Revised: December 06, 2023; Accepted: January 05, 2024

In this study, we hypothesized that microtextured titanium (Ti) surfaces produced by laser metal fusion (LMF) 3D printing may play an important role in osteoblastic differentiation of mesenchymal stem cells (MSCs). For that, MSCs derived from mouse bone marrow were cultured on Ti discs produced in two different ways: microtextured produced by acid etched (Ti-Ac, control group) and microtextured produced by LMF 3D printing (Ti-3D-LMF, test group), in which it was evaluated: (1) cell proliferation, (2) alkaline phosphatase activity and (3) extracellular matrix mineralization. The results showed that both groups allowed cell proliferation over time ( $p < 0.001$ ). Additionally, there were no statistically significant differences between groups in the assessments of alkaline phosphatase activity ( $p = 0.385$ ) and extracellular matrix mineralization ( $p = 0.234$ ). Although both groups evaluated induce cell proliferation and osteoblastic differentiation similarly, the technology used in the Ti-3D-LMF group may prove advantageous as it produces specific dental implants for patients through customization.

**Keywords:** Titanium, dental implant surface, 3D printing, laser metal fusion, acid etched, osteoblastic differentiation.

## 1. Introduction

Using implants for oral rehabilitation is the gold standard in dentistry, demonstrating predictable results and high success rates<sup>1-3</sup>. However, high success rates depend on several parameters, such as the biocompatibility of the material, characteristics of the surface, careful surgical procedure, general health conditions of the patient, and the local bone quality and quantity<sup>4,5</sup>.

The material of choice for manufacturing dental implants has been titanium (Ti), which can be commercially pure (cpTi) or associated with other metals in alloy form (Ti-6Al-4V). As an advantage, Ti has mechanical properties that support the functional load of mastication and, at the same time, it is biocompatible with bone tissue<sup>6-9</sup>. In the last years, several studies related to morphology, roughness, chemical composition, and wettability have sought to expand the range of possible applications of dental implants have been carried<sup>10-14</sup>. Despite numerous efforts to establish a correlation between the microstructure of the Ti implant, and biological responses at the cellular and molecular level, this point has not

yet been fully clarified. Modifications of surface roughness may have advantages of physical characteristics, resulting in new texturing that showed better results about anchorage strength in the early stages of osseointegration<sup>15,16</sup>.

Several technologies have been used to produce dental implants, with the machining process being the most used. However, research in the biomedical industry has been continuously working to improve the manufacturing process of these dental implants<sup>17</sup>. In this context, the method of manufacturing dental implants through additive manufacturing (AM), a technique already well-established in the aerospace industry, can be innovatively used in the implantology area<sup>18,19</sup>. The manufacture of dental implants can occur through a specific AM route called laser metal fusion (LMF) 3D printing<sup>20,21</sup>.

The LMF is based on the emission of a high-energy conical laser beam focused on a specific region of a thin layer of titanium powder, which melts according to the 3D layers projected by a computational model. This technology presents high precision, can be used for manufacturing dental implants with controlled porosity, mimicking the nature of bone tissue, and can optimize osseointegration by increasing surface hydrophilicity<sup>19,22,23</sup>.

\*e-mail: [gileade@ufg.br](mailto:gileade@ufg.br)

In this context, some studies have evaluated and demonstrated the advantages and applications of the LMF technique for the manufacture of dental implants<sup>19,23,24</sup>. CHENG and collaborators assessed the performance of the implants in an *in vitro* study and showed that the surface of implants produced by this technique increased the mineralized extracellular matrix of a human-derived cell line<sup>23</sup>. Another *in vitro* study demonstrated that dental implants manufactured using this technique alter the profile of the peri-implant microbiota, reducing the proportion of the red complex and decreasing the total counts of *Porphyromonas gingivalis*, which may be related to peri-implant disease<sup>24</sup>. In addition to these findings, an *in vivo* study in humans demonstrated that dental implant healing caps produced by this technique reduced the inflammatory infiltration around the peri-implant soft tissues<sup>19</sup>.

Based on the evidences above, this study aimed to evaluate the osteoblastic differentiation induced by microtextured titanium surface produced by LMF 3D printing (Ti-3D-LMF) compared to microtextured titanium surface produced by acid etching (Ti-Ac).

## 2. Materials and Methods

### 2.1. Ti samples

Commercially pure Ti discs, grade 2 (13 x 2 mm, Realum, São Paulo, SP, Brazil), were mechanically polished and washed with toluene in ultrasound. The Ti-Ac surface was used as a control group and obtained through treatment with acid etched with a solution containing HNO<sub>3</sub>, H<sub>2</sub>SO<sub>4</sub>, and HCl, as performed on commercially available osseointegrated dental implants<sup>25</sup>. Ti discs of Ti-3D-LMF, grade 5 (13 x 2 mm, Plenum, Jundiaí, SP, Brazil) were manufactured by LMF 3D printing technology, which is not described here because they are under industrial secrets. All discs were sterilized before use.

### 2.2. Characterization of the Ti surfaces

Ti discs (n=4) were examined in a Philips XL30 FEG scanning electron microscope (SEM, Japan) operated at 25 kV for surface topography characterization and their surface composition analysis was carried out using an energy-dispersive X-ray spectroscopy system (EDS, Bruker, USA) coupled to the microscope. The contact angle analysis (n=4) was performed using the static drop technique, using the Theta Flex Plus equipment (Biolin Scientific, Västra Frölunda, Sweden), in which a drop of 7 µL of distilled water was used and a standardized evaluation time of 30 seconds.

### 2.3. Cell culture

The MSCs were immortalized and characterized as previously described<sup>26</sup>. The iMSCs were cultured in a growth medium consisting of alpha-MEM (Gibco-Life Technologies, Waltham, MA, USA), supplemented with 20% v/v of fetal bovine serum (Gibco-Life Technologies), 1% v/v penicillin-streptomycin (Gibco - Life Technologies Waltham, MA, USA) and 0.3 µg/ml fungisone (Gibco-Life Technologies, Waltham, MA, USA) until subconfluence. Then, the iMSCs were plated on Ti-Ac and Ti-3D-LMF discs in 24-well plates (Corning Life

Sciences, Corning, NY, USA) at a density of 1x10<sup>4</sup> cells/disc and cultured in osteogenic medium, which was composed of growth medium supplemented with 5 µg/mL of ascorbic acid (Gibco-Life Technologies, Waltham, MA, USA), 7 mM beta-glycerophosphate (Sigma-Aldrich, San Luis, Missouri, USA) and dexamethasone 10<sup>-7</sup> M (Sigma-Aldrich San Luis, Missouri, USA) for of up to 17 days. The cultures were kept at 37°C in a humidified atmosphere containing 5% CO<sub>2</sub> and 95% atmospheric air, and the medium was changed every 48 hours.

### 2.4. Evaluation of cell proliferation

On days 3, 5, and 7, cell proliferation was determined by the colorimetric MTT assay {[3-(4,5-dimethylthiazol-2-yl)-2,5-diphenyltetrazolium bromide]}. For that, the culture medium was removed, and the wells washed with phosphate-buffered saline (PBS) solution (Gibco-Life Technologies Waltham, MA, USA) heated to 37 °C, filled with 1 mL of osteogenic medium containing 10% MTT (5 mg/mL) and incubated at 37 °C for 4 hours. After, the supernatants were aspirated, and the crystals were solubilized using 1 mL of an acidic isopropanol solution (HCl 0.04 N in isopropanol). The plates were shaken for 5 minutes, and a 150 µL aliquot from each well was transferred to a 96-well plate. Absorbance was evaluated using a µQuant spectrophotometer (BioTek Instruments Inc., Winooski, USA) using a wavelength of 570 nm. The data obtained in quintuplicate (n=5) were expressed by absorbance.

### 2.5. Evaluation of alkaline phosphatase (ALP) activity

On day 10, the ALP activity was evaluated through the release of thymolphthalein by hydrolysis of thymolphthalein monophosphate substrate, using a commercial kit according to the manufacturer's instructions (Labtest Diagnóstica, Lagoa Santa, MG, Brazil). The cell culture medium from the wells was removed to obtain cell lysates, and the Ti discs were washed with PBS. The wells were filled with 1 mL of 0.1% sodium lauryl sulfate solution (Sigma-Aldrich, San Luis, Missouri, USA). Samples were allowed to stand at room temperature for 30 minutes to promote cell lysis. Then, 50 µL of thymolphthalein monophosphate was mixed with 0.5 mL of 0.3 M diethanolamine buffer, pH 10.1, and left for 2 minutes at 37 °C. Afterward, an aliquot of 50 µL of the previously lysed sample was added, and this solution was kept at 37°C for 10 minutes. 2 mL of a 0.09 M Na<sub>2</sub>CO<sub>3</sub> and 0.25 M NaOH solution were added for color development. The absorbance was measured in a spectrophotometer (BioTek Instruments Inc. Winooski, VT, USA) using a wavelength of 590 nm. The data were obtained in quintuplicate (n=5). They were corrected by the standard provided by the manufacturer and normalized by the total protein.

Moreover, on day 10, ALP activity was evaluated using Fast Red staining. For this, the culture medium was removed. The Ti discs were washed with Hank's Solution (Hank's Balanced Salts, Sigma-Aldrich, Missouri, USA) heated to 37 °C and incubated with 1 mL of 120 mM Tris buffer solution (Sigma-Aldrich) containing 1.8 mM Fast Red TR (Sigma-Aldrich, Missouri, USA), naphthol-ASMX-phosphate (Sigma-Aldrich) at 0.9 mM and dimethylformamide (Merck, Darmstadt, Germany), for 30 minutes, in a humid atmosphere containing 5% CO<sub>2</sub> and 95% atmospheric air.

The wells were washed with PBS (Gibco-Life Technologies, Waltham, MA, USA) and photographed with a digital camera (Nikon, Japan). The data were obtained in quintuplicate ( $n=5$ ).

## 2.6. Evaluation of extracellular matrix mineralization

On day 17, the extracellular matrix mineralization was detected by staining with Alizarin red S (Sigma-Aldrich). The Ti discs were washed in Hanks' solution, fixed in 70% ethyl alcohol at 4 °C for 60 minutes, and washed in PBS. Then, they were stained with 2% Alizarin red S (Sigma-Aldrich), pH 4.2, at room temperature for 15 minutes, washed with PBS (Gibco-Life Technologies), and observed in a Leica DMLB fluorescence microscope (Leica, Germany). To quantitative results, 150  $\mu$ L of 10% acetic acid was added to each well, and the plates were kept under agitation for 30 minutes. The obtained solution was transferred to 1.5 mL tubes and vortexed for 30 seconds. Then, 100  $\mu$ L of mineral oil was added to the samples, which were kept at 85°C for 10 minutes and transferred to ice for 5 minutes. The tubes were centrifuged at 13.000 rpm for 15 minutes, and at the end, 40  $\mu$ L of 10% ammonium hydroxide was added. A volume of 150  $\mu$ L of the supernatant was used for reading in a  $\mu$ Quant spectrophotometer (BioTek Instruments Inc.) at a wavelength of 450 nm. The data were obtained in quintuplicate ( $n=5$ ) and expressed by absorbance.

## 2.7. Statistical analysis

The data from the cell proliferation assay were analyzed using the Two-Way ANOVA test, followed by Tukey's post-test, for comparisons between time, Ti-Ac (control group) and Ti-3D-LMF (test group). The data from ALP activity and extracellular matrix mineralization assay were analyzed using Student's t-test, for comparisons between Ti-Ac (control group) and Ti-3D-LMF (test group). The SigmaPlot program (Systat Software, San Jose, CA, USA) was used. The significance level adopted was 5% ( $p \leq 0.05$ ).

## 3. Results

### 3.1. Characterization of the Ti surfaces

The Ti-Ac group showed an irregular and homogeneous surface when analyzed at lower magnifications. It showed numerous concavities at higher magnifications, with pores on its surface at the micrometric scale level (Figures 1A, 1C, 1E).

When analyzed at lower magnifications, the Ti-3D-LMF group showed an irregular surface with a sphere and globular formation. It also showed numerous concavities at higher magnifications, with pores on its surface at the micrometer scale level. However, these pores were less numerous and deeper than the Ti-Ac group (Figures 1B, 1D, 1F).

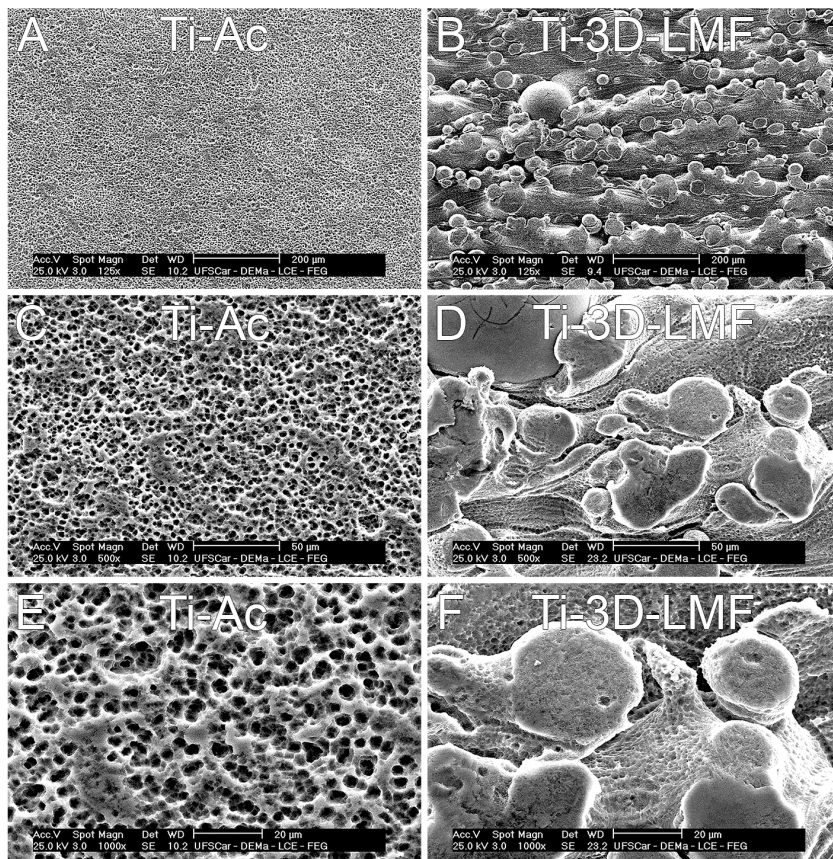


**Figure 1.** Surface characterization by Scanning Electron Microscope (SEM). The columns represent the groups of microtextured Ti discs produced by acid etching (Ti-Ac, A, C, E) and microtextured Ti discs produced by laser metal fusion 3D printing (Ti-3D-LMF, B, D, F). The lines represent the different SEM magnifications: 125x (A, B), 500x (C, D), and 1,000x (E, F).

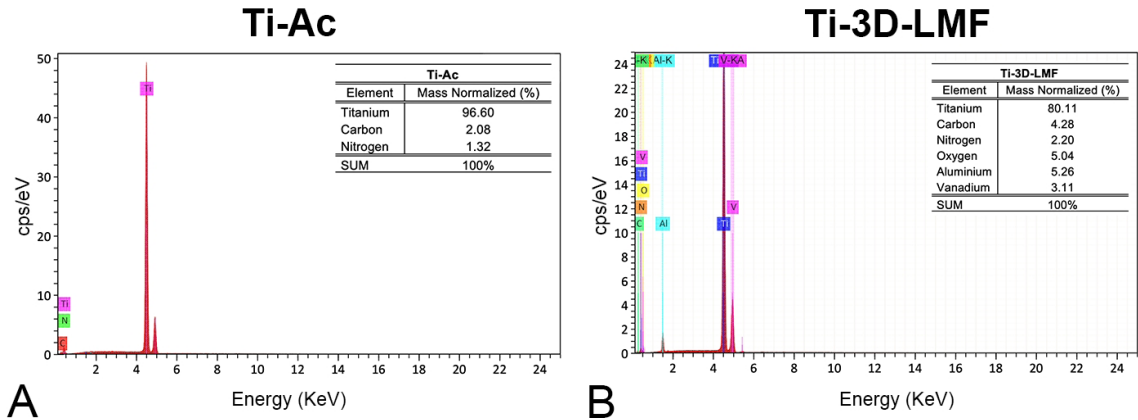


**Figure 2.** Surface characterization by Energy Dispersive X-ray Spectroscopy (EDS). Figure (A) represents the microtextured Ti discs produced by acid etching (Ti-Ac), and figure (B) represents microtextured Ti discs produced by laser metal fusion 3D printing (Ti-3D-LMF).

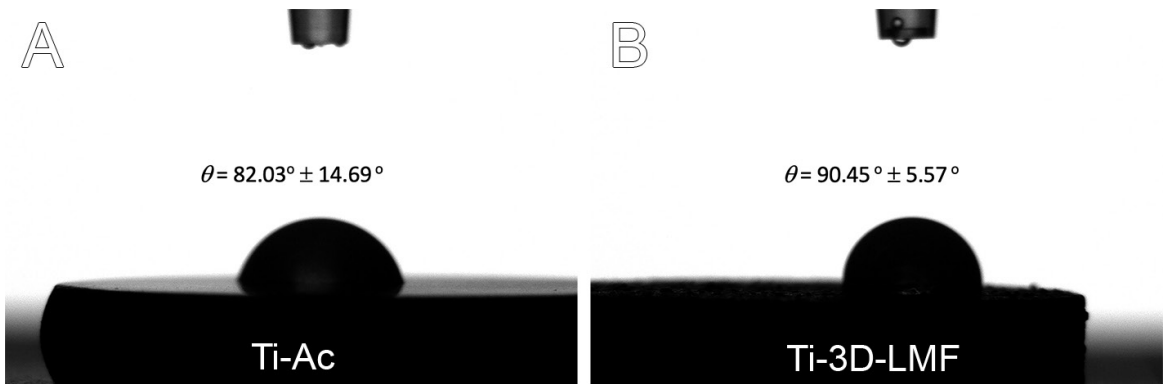


**Figure 3.** Surface characterization by wettability assay. Figure (A) represents the microtextured Ti discs produced by acid etching (Ti-Ac), and figure (B) represents microtextured Ti discs produced by laser metal fusion 3D printing (Ti-3D-LMF).

The analysis of the chemical composition, the Ti-Ac group showed 96.60% titanium, 2.08% carbon, and 1.32% nitrogen (Figure 2A). In comparison, the Ti-3D-LMF group showed the presence of 80.11% titanium, 4.28% carbon, 2.20% nitrogen, 5.04% oxygen, 5.26% aluminum, and 3.11% vanadium (Figure 2B).

The contact angle produced between the drop of distilled water and the surface on Ti-Ac was  $82.03^\circ \pm 14.69^\circ$  (Figure 3A), while on Ti-3D-LMF discs was  $90.45^\circ \pm 5.57^\circ$  (Figure 3B).

### 3.2. Evaluation of cell proliferation

The iMSCs grew and proliferated over time in both surfaces evaluated ( $p < 0.001$ ). However, there was no statistically significant difference in the number of cells between the Ti-Ac and Ti-3D-LMF groups at 3 and 5 days ( $p = 0.920$  and  $p = 0.486$ , respectively). Still, at 7 days, it was higher in the Ti-3D-LMF group compared to the Ti-Ac group ( $p < 0.001$ , Figure 4).

### 3.3. Evaluation of ALP activity

The ALP activity has shown no statistically significant difference between the Ti-Ac and Ti-3D-LMF groups at 10 days ( $p = 0.385$ , Figure 5).

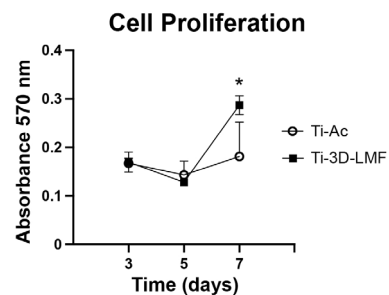


**Figure 4.** Cell proliferation on day 3, 5 and 7 of iMSCs cultivated in osteogenic medium on microtextured Ti discs produced by acid etching (Ti-Ac, control group) and microtextured Ti discs produced by laser metal fusion 3D printing (Ti-3D-LMF, test group). All data are presented as mean  $\pm$  standard deviation ( $n = 5$ ). \* indicates a statistically significant difference.

### 3.4. Evaluation of extracellular matrix mineralization

The extracellular matrix mineralization has shown no statistically significant difference between the Ti-Ac and Ti-3D-LMF groups at 17 days ( $p = 0.234$ , Figure 6).

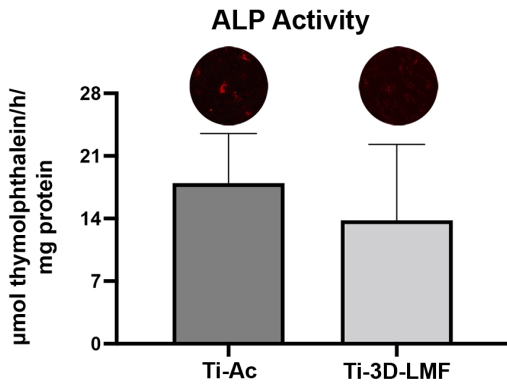


**Figure 5.** Alkaline phosphatase (ALP) activity on day 10 of iMSCs cultivated in osteogenic medium on microtextured Ti discs produced by acid etching (Ti-Ac, control group) and microtextured Ti discs produced by laser metal fusion 3D printing (Ti-3D-LMF, test group). The upper images show the in situ ALP activity, while the bar graph shows the ALP activity values obtained through the biochemical assay. All data are presented as mean  $\pm$  standard deviation (n=5).

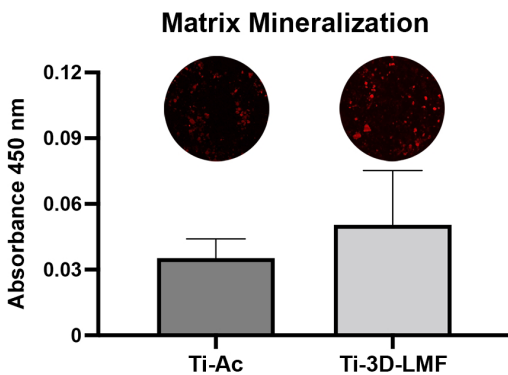


**Figure 6.** Extracellular matrix mineralization on day 17 of iMSCs cultivated in osteogenic medium on microtextured Ti discs produced by acid etching (Ti-Ac, control group) and microtextured Ti discs produced by laser metal fusion 3D printing (Ti-3D-LMF, test group). All data are presented as mean  $\pm$  standard deviation (n=5).

#### 4. Discussion

With the advancement of research in the biomedical industry, the manufacture of dental implants has evolved substantially, resulting in changes in the shape, composition, and surface. A classic approach and a simple method to obtain a roughness that mimics the bone structure and increases surface area, which favors osseointegration is a microtextured titanium surface produced by acid etching (Ti-Ac)<sup>27</sup>. However, the methods used to manufacture these dental implants have also evolved, with the process by LMF 3D printing, a recently-used technique. Therefore, in vitro studies to evaluate the osteoblast differentiation induced by surfaces produced through this technology are extremely important to guide dentists in choosing products for their patients, with predictable and low-cost results. In the present study, Ti-Ac and microtextured titanium surface produced by LMF 3D printing (Ti-3D-LMF) were characterized, and

iMSCs were cultured on both surfaces to evaluate osteoblastic differentiation by cell proliferation, ALP activity, and extracellular matrix mineralization. In general, the results showed that cell proliferation and osteoblastic differentiation were induced similarly in both groups regardless of the technique used in the manufacturing process.

The LMF 3D printing technology is already established in the aerospace industry and can be used in dentistry innovatively<sup>19</sup>. The advantages related to the manufacturing process of dental implants using this technology are flexibility in the design of the desired part (customization), energy efficiency, and improved functionality. In addition, compared to conventional production methods such as machined dental implants, the LMF 3D printing technique has lower processing costs, saving up to 40% by avoiding raw material waste<sup>28</sup>.

The analysis of SEM showed that the surface of the Ti-Ac group presented a homogeneous topography with numerous well-defined micro-concavities, and these results are corroborated by Lopes et al.<sup>29,30</sup> and Elias et al.<sup>25</sup>. The literature shows that the microtextured surface can facilitate the retention of osteogenic cells, favoring the adhesion of essential proteins for the osseointegration process<sup>31</sup>. When evaluating the surface of the Ti-3D-LMF group, a heterogeneous topography with the formation of spheres can be noticed. Corroborating this finding, Ahmed<sup>32</sup>, reports that the natural topography of the surface of titanium products produced by this technique regularly generates coarse spherical structures with concavities with a diameter of tens of microns on the surface. Taking these data together, regardless of the method used to produce the Ti discs and the differences in their topographies, both groups showed texturing on the micrometer scale.

The analysis of the chemical composition by EDS of the Ti-Ac group showed a high percentage of titanium (96.90%) and a low rate of carbon (2.08%) and nitrogen (1.32%). This result, in general, was already expected since commercially pure titanium grade 2 was used to manufacture the discs in this group. The presence of carbon and nitrogen identified during the EDS analysis can be explained, at least in part, as a contaminant from the machining process or during the acid etching<sup>30</sup>. The analysis of the chemical composition by EDS of the Ti-3D-LMF group showed a high percentage of titanium (80.11%), in addition to the presence of carbon (4.28%), nitrogen (2.20%), oxygen (5.04%), aluminum (5.26%) and vanadium (3.11%). These results were also expected since the discs were printed using a grade 5 titanium powder, Ti6Al4V alloy. It is noteworthy that the presence of oxygen can be explained, at least in part, by the formation of a layer of titanium dioxide (TiO<sub>2</sub>) caused by direct contact with atmospheric air<sup>33-35</sup>. As for the presence of aluminum and vanadium, this alloy has been widely used in the manufacture of prosthetic components and, in recent years, has been used for the manufacture of dental implants considered narrow, as they provide excellent mechanical properties, resistance to corrosion and biocompatibility<sup>36-39</sup>.

The contact angle analysis is defined as the angle of the intersection between the tangent line to the drop of distilled water and the solid surface<sup>40</sup>. This parameter is an essential tool for characterizing a surface as hydrophilic ( $\theta < 90^\circ$ )

or hydrophobic ( $\theta > 90^\circ$ )<sup>41</sup>. Hydrophilic surfaces promote better wettability, which contributes to a more significant adsorption of blood proteins and, consequently, impacts the osseointegration process<sup>42,43</sup>. Based on the findings of the present study, we can characterize the surface of the Ti-Ac group as hydrophilic ( $82.03^\circ \pm 14.69^\circ$ ) and the surface of the Ti-3D-LMF group as hydrophobic ( $90.45^\circ \pm 5.57^\circ$ ). However, it is important to point out that due to the standard deviation found during the evaluation of the last group, this classification borders on the category of hydrophilic surfaces.

The analysis of the cell proliferation by MTT has shown that, in general, both groups were favorable for such an event, demonstrating that both surfaces allowed cell adhesion without presenting cytotoxic characteristics. Besides, in most of the evaluated periods, the cell proliferation rate was similar between the Ti-Ac and Ti-3D-LMF groups. However, these results differ from those found by Hyzy et al.<sup>44</sup>, in which the authors showed a better cell proliferation rate in the LMF 3D printing group.

Alkaline phosphatase is an essential enzyme in osteoblastic differentiation and bone mineralization<sup>45</sup>. After the proliferative phase (days from 1 to 4), starts the early cell differentiation characterized by matrix maturation (days from 5 to 14), which the cells start expressing ALP and after an initial peak, ALP level tends to decline in the final stage (days from 14 to 28), characterized by mineralization<sup>46</sup>. Indeed, Stein et al.<sup>47</sup>, showed that the temporal expression of ALP during the development of the osteoblast phenotype in vitro was low around 7 days and increased over time. The peak of its activity in MSCs is detected in the intermediate stages of the osteoblastic differentiation process, ranging from 7 to 14 days<sup>48</sup>. Therefore, we believe that 10 days is a period in which there should be more differences in ALP activity induced by the surfaces evaluated.

In the present study, we evaluated the activity of this enzyme both in situ to evaluate its activity in the cell membrane (extracellular) and through the biochemical method to evaluate its activity in the cytoplasm (intracellular), as demonstrated by Birmingham et al.<sup>49</sup>. Our results show that the techniques used effectively detect ALP activity in iMSCs, and both groups induced ALP activity at the same intensity, indicating that in the evaluated period, the iMSCs were in the process of osteoblastic differentiation.

Additionally, when we evaluated extracellular matrix mineralization, a phenomenon linked to the final stage of the osteoblastic differentiation process<sup>48</sup>, we also observed the similarity of both groups to induce such a process, with a trend to be higher on Ti-3D-LMF group. This finding is similar to the findings by Cheng et al.<sup>23</sup>, in which the authors show that the LMF 3D printing technique increased the production of mineralized extracellular matrix of a human-derived cell line. The extracellular matrix mineralization was evaluated at 17 days because the mineralization phase starts on day 14, and studies using titanium surfaces performed the mineralization assay at this time point<sup>46,50</sup>. In agreement with these studies, despite no differences observed between Ti-Ac and Ti-3D-LMF this study showed the cultures on both surfaces with intense staining of the mineralized nodules at 17 days, which is indicative of hydroxyapatite deposition.

Some studies were carried out to understand how the microtexturized Ti surfaces stimulate the process of osteoblastic differentiation and, consequently, osseointegration. As for the Ti-Ac group, its osteogenic potential is related to the fact that its surface stimulates the integrin cell signaling pathway through beta-3 integrin and via focal adhesion kinases<sup>29,30</sup>. As for the Ti-3D-LMF group, its osteogenic potential is related to its surface stimulating the production of growth factors such as vascular endothelial growth factor (VEGF) and bone morphogenic protein 2 (BMP-2)<sup>51</sup>. However, the intracellular mechanisms of the interaction between MSCs and the surface of both groups still need to be fully elucidated, requiring further studies for the complete understanding and improvement of these biomaterials in the medical and dental areas.

In conclusion, considering the translational research, our study is a first step of the basic effects of a microtextured titanium surface produced by LMF 3D printing on osteoblastic differentiation, and our results reveal that the manufacturing process generated differences in the surface topographies of Ti-Ac and Ti-3D-LMF groups. However, it could not generate differences in cell proliferation and osteoblastic differentiation of iMSCs.

## 5. Acknowledgments

The authors thank the Bone Research Lab (School of Dentistry of Ribeirão Preto, University of São Paulo) and the Laboratory of Structural Characterization (LCE, Federal University of São Carlos) for the general facilities.

## 6. References

1. Tamer Y, Özcan I. Comparison of implant survival rates and biologic and mechanical complications with implant-supported fixed complete dental prostheses using four and six implants. *Int J Periodontics Restorative Dent.* 2023;43(4):e157-63. <http://dx.doi.org/10.11607/prd.5997>.
2. Papaspyridakos P, Mokti M, Chen CJ, Benic GI, Gallucci GO, Chronopoulos V. Implant and prosthodontic survival rates with implant fixed complete dental prostheses in the edentulous mandible after at least 5 years: a systematic review. *Clin Implant Dent Relat Res.* 2014;16(5):705-17. <http://dx.doi.org/10.1111/cid.12036>.
3. Wennerberg A, Albrektsson T. Current challenges in successful rehabilitation with oral implants. *J Oral Rehabil.* 2011;38(4):286-94. <http://dx.doi.org/10.1111/j.1365-2842.2010.02170.x>.
4. Parihar AS, Singh R, Vaibhav V, Kumar K, Singh R, Jerry JJ. 10 years retrospective study of assessment of prevalence and risk factors of dental implants failures. *J Family Med Prim Care.* 2020;9(3):1617-9. [http://dx.doi.org/10.4103/jfmpc.jfmpc\\_1171\\_19](http://dx.doi.org/10.4103/jfmpc.jfmpc_1171_19).
5. Elias CN, Oshida Y, Lima JH, Muller CA. Relationship between surface properties (roughness, wettability and morphology) of titanium and dental implant removal torque. *J Mech Behav Biomed Mater.* 2008;1(3):234-42. <http://dx.doi.org/10.1016/j.jmbbm.2007.12.002>.
6. Silva RCS, Agreli A, Andrade AN, Mendes-Marques CL, Arruda IRS, Santos LRL, et al. Titanium dental implants: an overview of applied nanobiotechnology to improve biocompatibility and prevent infections. *Materials.* 2022;15(9):3150. <http://dx.doi.org/10.3390/ma15093150>.
7. Bosshardt DD, Chappuis V, Buser D. Osseointegration of titanium, titanium alloy and zirconia dental implants: current knowledge and open questions. *Periodontol 2000.* 2017;73(1):22-40. <http://dx.doi.org/10.1111/prd.12179>.

8. Sverzut AT, Albuquerque GC, Crippa GE, Chiesa R, Della Valle C, Oliveira PT, et al. Bone tissue, cellular, and molecular responses to titanium implants treated by anodic spark deposition. *J Biomed Mater Res A*. 2012;100A(11):3092-8. <http://dx.doi.org/10.1002/jbm.a.34249>.
9. Brånemark PI. Osseointegration and its experimental background. *J Prosthet Dent*. 1983;50(3):399-410. [http://dx.doi.org/10.1016/S0022-3913\(83\)80101-2](http://dx.doi.org/10.1016/S0022-3913(83)80101-2).
10. Fahlstedt P, Wennerberg A, Bunaes DF, Lie SA, Leknes KN. Dental implant surface morphology, chemical composition, and topography following double wavelength (2780/940 nm) laser irradiation. An in vitro study. *Clin Exp Dent Res*. 2023;9(1):25-35. <http://dx.doi.org/10.1002/cre2.709>.
11. Ferraz EP, Sverzut AT, Freitas GP, Sá JC, Alves C Jr, Beloti MM, et al. Bone tissue response to plasma-nitrided titanium implant surfaces. *J Appl Oral Sci*. 2015;23(1):9-13. <http://dx.doi.org/10.1590/1678-775720140376>.
12. Ayobian-Markazi N, Karimi M, Safar-Hajhosseini A. Effects of Er: YAG laser irradiation on wettability, surface roughness, and biocompatibility of SLA titanium surfaces: an in vitro study. *Lasers Med Sci*. 2015;30(2):561-6. <http://dx.doi.org/10.1007/s10103-013-1361-y>.
13. Freitas GP, Lopes HB, Martins-Neto EC, Oliveira PT, Beloti MM, Rosa AL. Effect of surface nanotopography on bone response to titanium implant. *J Oral Implantol*. 2016;42(3):240-7. <http://dx.doi.org/10.1563/aaaid-joi-D-14-00254>.
14. Elias CN, Rocha FA, Nascimento AL, Coelho PG. Influence of implant shape, surface morphology, surgical technique and bone quality on the primary stability of dental implants. *J Mech Behav Biomed Mater*. 2012;16:169-80. <http://dx.doi.org/10.1016/j.jmbmm.2012.10.010>.
15. Albrektsson T, Wennerberg A. On osseointegration in relation to implant surfaces. *Clin Implant Dent Relat Res*. 2019;21(Suppl 1):4-7. <http://dx.doi.org/10.1111/cid.12742>.
16. Zhang W, Wang G, Liu Y, Zhao X, Zou D, Zhu C, et al. The synergistic effect of hierarchical micro/nano-topography and bioactive ions for enhanced osseointegration. *Biomaterials*. 2013;34(13):3184-95. <http://dx.doi.org/10.1016/j.biomaterials.2013.01.008>.
17. Hoque ME, Showva NN, Ahmed M, Rashid AB, Sadique SE, El-Bialy T, et al. Titanium and titanium alloys in dentistry: current trends, recent developments, and future prospects. *Heliyon*. 2022;8(11):e11300. <http://dx.doi.org/10.1016/j.heliyon.2022.e11300>.
18. Huang S, Wei H, Li D. Additive manufacturing technologies in the oral implant clinic: a review of current applications and progress. *Front Bioeng Biotechnol*. 2023;11:1100155. <http://dx.doi.org/10.3389/fbioe.2023.1100155>.
19. Mangano C, Mangano FG, Shibli JA, Roth LA, d'Addazio G, Piattelli A, et al. Immunohistochemical evaluation of peri-implant soft tissues around machined and Direct Metal Laser Sintered (DMLS) healing abutments in humans. *Int J Environ Res Public Health*. 2018;15(8):1611. <http://dx.doi.org/10.3390/ijerph15081611>.
20. Hernández-Nava E, Mahoney P, Smith CJ, Donoghue J, Todd I, Tammas-Williams S. Additive manufacturing titanium components with isotropic or graded properties by hybrid electron beam melting/hot isostatic pressing powder processing. *Sci Rep*. 2019;9(1):4070. <http://dx.doi.org/10.1038/s41598-019-40722-3>.
21. Liaw CY, Guvendiren M. Current and emerging applications of 3D printing in medicine. *Biofabrication*. 2017;9(2):024102. <http://dx.doi.org/10.1088/1758-5090/aa7279>.
22. Calazans JV No, Reis ACD, Valente MLDC. Osseointegration in additive-manufactured titanium implants: a systematic review of animal studies on the need for surface treatment. *Heliyon*. 2023;9(6):e17105. <http://dx.doi.org/10.1016/j.heliyon.2023.e17105>.
23. Cheng A, Cohen DJ, Boyan BD, Schwartz Z. Laser-sintered constructs with bio-inspired porosity and surface micro/nano-roughness enhance mesenchymal stem cell differentiation and matrix mineralization in vitro. *Calcif Tissue Int*. 2016;99(6):625-37. <http://dx.doi.org/10.1007/s00223-016-0184-9>.
24. Pinguero J, Piattelli A, Paiva J, Figueiredo LC, Feres M, Shibli J, et al. Additive manufacturing of titanium alloy could modify the pathogenic microbial profile: an in vitro study. *Braz Oral Res*. 2019;33(Suppl 1):e065. <http://dx.doi.org/10.1590/1807-3107bor-2019.vol33.0065>.
25. Elias CN, Gravina PA, Silva CE Fo, Nascente PA. Preparation of bioactive titanium surfaces via fluoride and fibronectin retention. *Int J Biomater*. 2012;2012:290179. <http://dx.doi.org/10.1155/2012/290179>.
26. Freitas GP, Lopes HB, Souza ATP, Gomes MPO, Quiles GK, Gordon J, et al. Mesenchymal stem cells overexpressing BMP-9 by CRISPR-Cas9 present high in vitro osteogenic potential and enhance in vivo bone formation. *Gene Ther*. 2021;28(12):748-59. <http://dx.doi.org/10.1038/s41434-021-00248-8>.
27. Giner L, Mercadé M, Torrent S, Punset M, Pérez RA, Delgado LM, et al. Double acid etching treatment of dental implants for enhanced biological properties. *J Appl Biomater Funct Mater*. 2018;16(2):83-9. <http://dx.doi.org/10.5301/jabfm.5000376>.
28. Magalhães OA, de Alcantara RJA, Gomes JAP, Caiado de Castro J No, Schor P. Titanium powder 3D-printing technology for a novel keratoprosthesis in alkali-burned rabbits. *Transl Vis Sci Technol*. 2022;11(8):14. <http://dx.doi.org/10.1167/tvst.11.8.14>.
29. Lopes HB, Souza ATP, Freitas GP, Elias CN, Rosa AL, Beloti MM. Effect of focal adhesion kinase inhibition on osteoblastic cells grown on titanium with different topographies. *J Appl Oral Sci*. 2020;28:e20190156. <http://dx.doi.org/10.1590/1678-7757-2019-0156>.
30. Lopes HB, Freitas GP, Elias CN, Tye C, Stein JL, Stein GS, et al. Participation of integrin  $\beta 3$  in osteoblast differentiation induced by titanium with nano or microtopography. *J Biomed Mater Res A*. 2019;107(6):1303-13. <http://dx.doi.org/10.1002/jbm.a.36643>.
31. Rodriguez-González R, Monsalve-Guil L, Jimenez-Guerra A, Velasco-Ortega E, Moreno-Muñoz J, Nuñez-Marquez E, et al. Relevant aspects of titanium topography for osteoblastic adhesion and inhibition of bacterial colonization. *Materials*. 2023;16(9):3553. <http://dx.doi.org/10.3390/ma16093553>.
32. Ahmed N. Direct metal fabrication in rapid prototyping: a review. *J Manuf Process*. 2019;42:167-91. <http://dx.doi.org/10.1016/j.jmapro.2019.05.001>.
33. Yeo IL. Modifications of dental implant surfaces at the micro- and nano-level for enhanced osseointegration. *Materials*. 2019;13(1):89. <http://dx.doi.org/10.3390/ma13010089>.
34. Yi J, Bernard C, Variola F, Zalzal SF, Wuest JD, Rosei F, et al. Characterization of a bioactive nanotextured surface created by controlled chemical oxidation of titanium. *Surf Sci*. 2006;600(19):4613-21. <http://dx.doi.org/10.1016/j.susc.2006.07.053>.
35. Sittig C, Textor M, Spencer ND, Wieland M, Vallotton PH. Surface characterization of implant materials c.p. Ti, Ti-6Al-7Nb and Ti-6Al-4V with different pretreatments. *J Mater Sci Mater Med*. 1999;10(1):35-46. <http://dx.doi.org/10.1023/A:1008840026907>.
36. Cordeiro JM, Barão VAR. Is there scientific evidence favoring the substitution of commercially pure titanium with titanium alloys for the manufacture of dental implants? *Mater Sci Eng C*. 2017;71:1201-15. <http://dx.doi.org/10.1016/j.msec.2016.10.025>.
37. Shah FA, Trobos M, Thomsen P, Palmquist A. Commercially pure titanium (cp-Ti) versus titanium alloy (Ti6Al4V) materials as bone anchored implants: is one truly better than the other? *Mater Sci Eng C*. 2016;62:960-6. <http://dx.doi.org/10.1016/j.msec.2016.01.032>.
38. Barão VA, Mathew MT, Assunção WG, Yuan JC, Wimmer MA, Sukotjo C. Stability of cp-Ti and Ti-6Al-4V alloy for dental implants as a function of saliva pH - an electrochemical study. *Clin Oral Implants Res*. 2012;23(9):1055-62. <http://dx.doi.org/10.1111/j.1600-0501.2011.02265.x>.
39. McCracken M. Dental implant materials: commercially pure titanium and titanium alloys. *J Prosthodont*. 1999;8(1):40-3. <http://dx.doi.org/10.1111/j.1532-849X.1999.tb00006.x>.

40. Mekayarajjanonoth T, Winkler S. Contact angle measurement on dental implant biomaterials. *J Oral Implantol.* 1999;25(4):230-6. [http://dx.doi.org/10.1563/1548-1336\(1999\)025<0230:CAMO DI>2.3.CO;2](http://dx.doi.org/10.1563/1548-1336(1999)025<0230:CAMO DI>2.3.CO;2).
41. Strnad G, Chirila N, Petrovan C, Russu O. Contact angle measurement on medical implant titanium based biomaterials. *Procedia Technol.* 2016;22:946-53. <http://dx.doi.org/10.1016/j.protcy.2016.01.094>.
42. Rupp F, Liang L, Geis-Gerstorfer J, Scheideler L, Hüttig F. Surface characteristics of dental implants: a review. *Dent Mater.* 2018;34(1):40-57. <http://dx.doi.org/10.1016/j.dental.2017.09.007>.
43. Gittens RA, Scheideler L, Rupp F, Hyzy SL, Geis-Gerstorfer J, Schwartz Z, et al. A review on the wettability of dental implant surfaces II: biological and clinical aspects. *Acta Biomater.* 2014;10(7):2907-18. <http://dx.doi.org/10.1016/j.actbio.2014.03.032>.
44. Hyzy SL, Cheng A, Cohen DJ, Yatzkaier G, Whitehead AJ, Clohessy RM, et al. Novel hydrophilic nanostructured microtexture on direct metal laser sintered Ti-6Al-4V surfaces enhances osteoblast response in vitro and osseointegration in a rabbit model. *J Biomed Mater Res A.* 2016;104(8):2086-98. <http://dx.doi.org/10.1002/jbm.a.35739>.
45. Sekaran S, Vimalraj S, Thangavelu L. The physiological and pathological role of tissue nonspecific alkaline phosphatase beyond mineralization. *Biomolecules.* 2021;11(11):1564. <http://dx.doi.org/10.3390/biom11111564>.
46. Carluccio M, Ziberi S, Zuccarini M, Giuliani P, Caciagli F, Di Iorio P, et al. Adult mesenchymal stem cells: is there a role for purine receptors in their osteogenic differentiation? *Purinergic Signal.* 2020;16(3):263-87. <http://dx.doi.org/10.1007/s11302-020-09703-4>.
47. Stein GS, Lian JB, Owen TA. Relationship of cell growth to the regulation of tissue-specific gene expression during osteoblast differentiation. *FASEB J.* 1990;4(13):3111-23. <http://dx.doi.org/10.1096/fasebj.4.13.2210157>.
48. Amarasekara DS, Kim S, Rho J. Regulation of osteoblast differentiation by cytokine networks. *Int J Mol Sci.* 2021;22(6):2851. <http://dx.doi.org/10.3390/ijms22062851>.
49. Birmingham E, Niebur GL, McHugh PE, Shaw G, Barry FP, McNamara LM. Osteogenic differentiation of mesenchymal stem cells is regulated by osteocyte and osteoblast cells in a simplified bone niche. *Eur Cell Mater.* 2012;23:13-27. <http://dx.doi.org/10.22203/eCM.v023a02>.
50. Petri AD, Teixeira LN, Crippa GE, Beloti MM, Oliveira PT, Rosa AL. Effects of low-level laser therapy on human osteoblastic cells grown on titanium. *Braz Dent J.* 2010;21(6):491-8. <http://dx.doi.org/10.1590/S0103-64402010000600003>.
51. Mangano C, De Rosa A, Desiderio V, d'Aquino R, Piattelli A, De Francesco F, et al. The osteoblastic differentiation of dental pulp stem cells and bone formation on different titanium surface textures. *Biomaterials.* 2010;31(13):3543-51. <http://dx.doi.org/10.1016/j.biomaterials.2010.01.056>.